Accepted Manuscript

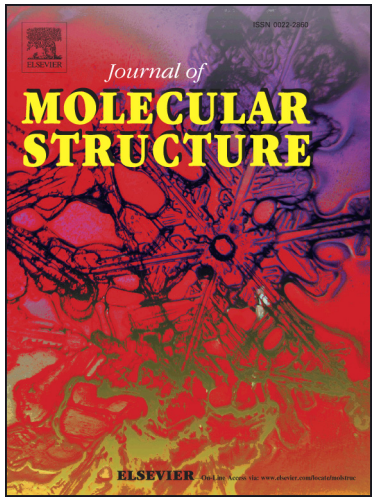

Studies on the Self-catalysed Knoevenagel Condensation, Characterization, DPPH Radical Scavenging Activity, Cytotoxicity, and Molecular Properties of 5-Arylidene-2,2-dimethyl-1,3-dioxane-4,6-diones using Single Crystal XRD and DFT Techniques

G.S. Suresh Kumar, A. Antony Muthu Prabhu, N. Bhuvanesh

PII: S0022-2860(14)00678-4
DOI: http://dx.doi.org/10.1016/j.molstruc.2014.06.065
Reference: MOLSTR 20746

To appear in: *Journal of Molecular Structure*

Received Date: 8 March 2014
Revised Date: 22 June 2014
Accepted Date: 22 June 2014

Please cite this article as: G.S. Suresh Kumar, A. Antony Muthu Prabhu, N. Bhuvanesh, Studies on the Self-catalysed Knoevenagel Condensation, Characterization, DPPH Radical Scavenging Activity, Cytotoxicity, and Molecular Properties of 5-Arylidene-2,2-dimethyl-1,3-dioxane-4,6-diones using Single Crystal XRD and DFT Techniques, *Journal of Molecular Structure* (2014), doi: http://dx.doi.org/10.1016/j.molstruc.2014.06.065

Studies on the Self-catalysed Knoevenagel Condensation, Characterization, DPPH Radical Scavenging Activity, Cytotoxicity, and Molecular Properties of 5-Arylidene-2,2-dimethyl-1,3-dioxane-4,6-diones using Single Crystal XRD and DFT Techniques

G.S. Suresh Kumar[a,*], A. Antony Muthu Prabhu[b], and N. Bhuvanesh[c]

[a]*Faculty of Chemistry, Department of Science and Humanities, Dr. Mahalingam College of Engineering and Technology (Dr. MCET), Udumalai Road, Pollachi 642 003, Tamilnadu, India.*
[b]*Department of Chemistry, Manonmaniam Sundaranar University, Tirunelveli 627 012, Tamilnadu, India.*
[c]*Department of Chemistry, Texas A & M University, College Station, Texas 77842, USA.*

Abstract

We have studied the self-catalysed Knoevenagel condensation, spectral characterization, DPPH radical scavenging activity, cytotoxicity, and molecular properties of 5-arylidene-2,2-dimethyl-1,3-dioxane-4,6-diones using single crystal XRD and DFT techniques. In the absence of any catalyst, a series of novel 5-arylidene-2,2-dimethyl-1,3-dioxane-4,6-diones were synthesized using Meldrum's acid and formylphenoxyaliphatic acid(s) in water. These molecules are arranged in the dimer form through intermolecular H-bonding in the single crystal XRD structure. Compounds have better DPPH radical scavenging activity and cytotoxicity against A431 cancer cell line. The optimized molecular structure, natural bond orbital analysis, electrostatic potential map, HOMO-LUMO energies, molecular properties, and atomic charges of these molecules have been studied by performing DFT/B3LYP/3-21G(*) level of theory in gas phase.

Keywords: Knoevenagel condensation, Meldrum's acid, formylphenoxyaliphatic acid, SCXRD, MEP, NBO

Corresponding author: e-mail: shunsureshkumar@gmail.com,

phone no: +9190031 80667

Highlights

- Phenoxyaliphatic acids act as a self-catalyst for the Knoevenagel condensation reaction.
- Phenoxyaliphatic acids of ylidene derivatives show better radical scavenging activity.
- Compounds are stabilized by H-bonding; 2c alone shows π-π interactions.
- NBO analysis, the interaction energy of 2a and 2b is higher than that of 2c and 2d.
- Intermolecular interactions are studied using MEP analysis.
- HOMO-LUMO energy gap confirms that the highest stability of compounds.

Graphical abstract

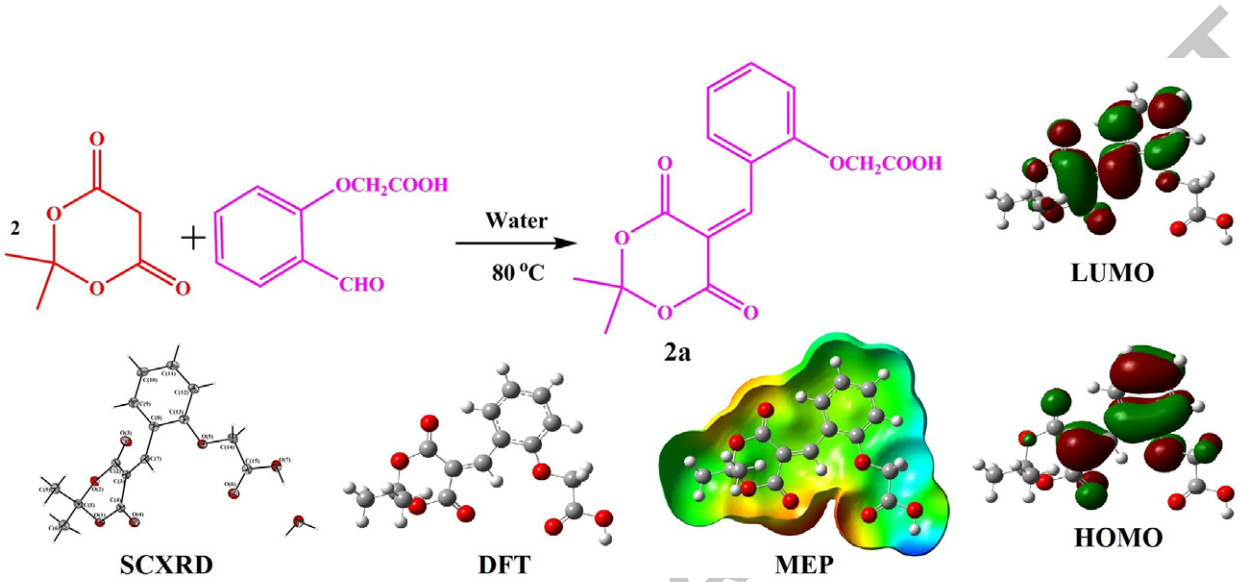

1. Introduction

The calculation of wide range of molecular properties with DFT allows a close connection between experiment and theory. DFT studies can complement experimental investigations, or even venture with some confidence into experimentally unexplored territory [1]. B3LYP/3-21G(*) method has been successfully used to predict the molecular properties of simple to supramolecular systems [2].

Knoevenagel condensation of Meldrum's acid and aldehydes gives rise to corresponding ylidene derivatives. The ylidene derivatives obtained are versatile substrates for variety of reactions [3]. Knoevenagel condensation of aldehydes and Meldrum's acid is generally catalysed by bases [4] such as pyridine or by piperidine/glacial acetic acid in benzene with water removal [5], anhydrous zinc chloride was reported to promote the reaction in the absence of any solvent [6], uncatalysed reaction was reported in the literature using DMF or DMSO [7], and water [8]. A cationic coordination cage dramatically accelerating the Knoevenagel condensation of aromatic aldehydes in water under neutral conditions was reported by Murase *et al* [9].

Aryloxyaliphatic acids are among the most vital moieties which are associated with potent antimicrobial, antidiabetic, antibiotic, anti-obesity, diagnostic, anticancer, radical scavenging, inhibition of platelet aggregation activities *etc* [10].

The *in-situ* Bronsted-Lowry acid catalytic behaviour of formylphenoxyaliphatic acid(s) for the syntheses of bis(indolyl)methanes and xanthenes were studied by us [11, 12]. The present work, we extend the catalytic behaviour of formylphenoxyaliphatic acid(s) to Knoevenagel condensation of Meldrum's acid and formylphenoxyaliphatic acid(s) in water without any catalyst. DPPH radical scavenging activity and cytotoxicity of the newly synthesized ylidene derivatives are screened out. The molecular properties of the ylidene derivatives are studied using single crystal XRD and DFT method.

2. Experimental

2.1. General Methods

Melting points were measured in open capillary tubes and are uncorrected. Infrared spectra were recorded on a JASCO FT-IR Model 410 spectrophotometer (in KBr pellet). Band positions are reported in reciprocal centimetres (cm^{-1}). The ^{1}H NMR and ^{13}C NMR spectra were recorded on a Bruker (Avance) 500 MHz NMR instrument using TMS as internal standard and $CDCl_3$ as solvent. Standard Bruker software was used throughout. Chemical shifts are given in parts per million (δ scale) and the coupling constants in Hertz. Silica gel-G plates (Merck) were used for TLC analysis with a mixture of chloroform and methanol as eluent. The electrospray (ESI) mass spectra were recorded on a THERMO Finnigan LCQ Advantage max ion trap mass spectrometer. Samples (10 μL) (dissolved in solvent such as methanol/acetonitrile/water) were introduced into the ESI source through Finnigan surveyor autosampler. Elemental analyses were performed on a Perkin Elmer 2400 Series II Elemental CHNS analyzer. Formylphenoxyacetic acids were synthesized by literature method [13].

2.2. General Syntheses of 5-Arylidene-2,2-dimethyl-1,3-dioxane-4,6-dione (2)

Formylphenoxyaliphatic acid (2.5 mmol) was dissolved in water (10 mL) at 80 ^{o}C, Meldrum's acid (2.5 mmol) was added with vigorous stirring at 80 ^{o}C. After the completion of the reaction (monitored by TLC, chloroform:methanol), the reaction mixture was cooled to room temperature, the solid was filtered, washed with water, dried well, and recrystallized from hot aqueous ethanol. Newly synthesized compounds were characterized by single crystal XRD, IR, NMR, and Mass analysis.

2-{2-[(2,2-dimethyl-4,6-dioxo-1,3-dioxan-5-ylidene)methyl]phenoxy}acetic acid (2a).

Green solid; 88%; m.p. 189-191^{o}C; IR (KBr): 1754, 1716, 1597, 1588 cm^{-1}; ^{1}H NMR (300 MHz,

δ ppm): 1.77 (6H, s), 4.87 (2H, s), 7.05 (2H, m), 7.54 (1H, J=7.5 Hz, t), 7.84 (1H, J=7.8 Hz, d), 8.62 (1H, s); ^{13}C NMR (75 MHz, δ ppm): 27.5, 65.7, 104.9, 112.9, 116.2, 121.0, 121.7, 132.3, 134.9, 151.9, 157.9, 159.8, 162.7, 170.0; ESI-MS: 305.08; Anal.Calcd. for $C_{26}H_{22}N_2O_4$: C, 58.82; H, 4.61%. Found: C, 59.64; H, 4.25%.

2-{4-[(2,2-dimethyl-4,6-dioxo-1,3-dioxan-5-ylidene)methyl]phenoxy}acetic acid (2b). Green solid; 92%; m.p. 176-178^{o}C; IR (KBr): 1735, 1717, 1569, 1553 cm^{-1}; ^{1}H NMR (300 MHz, δ ppm): 1.74 (6H, s), 4.86 (2H, s), 7.07 (2H, J=8.5 Hz, d), 8.20 (2H, J=8.5 Hz, d), 8.31 (1H, s); ^{13}C NMR (75 MHz, δ ppm): 27.3, 65.0, 104.6, 112.3, 115.1, 125.3, 137.2, 156.8, 160.5, 162.8, 163.5, 169.9; ESI-MS: 305.00; Anal.Calcd. for $C_{26}H_{22}N_2O_4$: C, 58.82; H, 4.61%. Found: C, 58.24; H, 4.52%.

3-{2-[(2,2-dimethyl-4,6-dioxo-1,3-dioxan-5-ylidene)methyl]phenoxy}propanoic acid (2c). Green solid; 90%; m.p. 202-204^{o}C; IR (KBr): 1752, 1723, 1599 cm^{-1}; ^{1}H NMR (300 MHz, δ ppm): 1.75 (6H, s), 2.73 (2H, J=5.1Hz, t), 4.28 (2H, J=5.4 Hz, t), 7.02 (1H, J=8.1 Hz, t), 7.17 (1H, J=8.1Hz, t), 7.54 (1H, J=7.5Hz, d), 7.77 (1H, J=7.5 Hz, d), 8.46 (1H, s); ^{13}C NMR (75 MHz, δ ppm): 27.5, 34.2, 64.9, 104.9, 112.8, 116.1, 120.6, 121.4, 124.7, 127.8, 132.4, 135.1, 140.4, 151.8, 158.4, 158.7, 159.8, 162.7, 172.3; ESI-MS: 319.17; Anal.Calcd. for $C_{26}H_{22}N_2O_4$: C, 58.82; H, 4.61%. Found: C, 58.64; H, 4.82%.

3-{4-[(2,2-dimethyl-4,6-dioxo-1,3-dioxan-5-ylidene)methyl]phenoxy}propanoic acid (2d). Green solid; 90%; m.p. 202-204^{o}C; IR (KBr): 1748, 1720, 1579, 1558 cm^{-1}; ^{1}H NMR (300 MHz, δ ppm): 1.74 (6H, s), 2.75 (2H, J=1.8Hz, t), 4.31 (2H, J=1.8 Hz, t), 7.10 (2H, J=8.0 Hz, d), 8.22 (2H, J=8.0Hz, d), 8.32 (1H, s); ^{13}C NMR (75 MHz, δ ppm): 27.3, 34.2, 64.7, 104.5, 111.9, 115.1, 115.3, 124.9, 137.5, 156.9, 160.5, 163.5, 163.6, 172.4; ESI-MS: 319.08; Anal.Calcd. for $C_{26}H_{22}N_2O_4$: C, 58.82; H, 4.61%. Found: C, 59.32; H, 4.68%.

2.3. X-ray structure determination

Single crystals were determined using a BRUKER APEX 2 X-ray (three-circle) diffractometer. The data reduction was done with the program APEX2 [14]. The absorption correction was employed using the program SADABS [14]. The structure solution was obtained using SHELXTL (XS) [15] and refined on F2 to convergence [16,17]. Absence of additional symmetry was verified using PLATON (ADDSYM).

2.4. DPPH Free Radical Scavenging Activity

The free radical scavenging activity of the compounds was measured by the decrease in absorbance of methanolic solution of DPPH [18]. A stock solution of DPPH (33 mg/L) was prepared in methanol and 5 mL of this solution was added to 1 mL of each compound at different concentrations (25, 50 µg/mL). After 30 min, absorbance was measured at 517 nm. Scavenging activity was expressed as the percentage inhibition.

2.5. In vitro Anticancer Activity

The human skin epithelial cell carcinoma cell line (A431), human stomach adenocarcinoma cancer cell line (AGS), and glioblastoma cell line (U373MG) were obtained from National Centre for Cell Science (NCCS), Pune and grown in Dulbecco's Modified Eagle Medium (DMEM) containing 10% fetal bovine serum (FBS). All cells were maintained at 37^{o}C, 5% CO_2, 95% air, and 100% relative humidity. Maintenance cultures were passaged weekly and the culture medium was changed twice a week. Anticancer activity was done as per our earlier report [11, 12].

2.6. Computational methods

The density functional theory (DFT/B3LYP) at the 3-21G(*) basis set level was adopted to calculate the properties of all these molecules in the present work. All the calculations were performed using Gaussian 09W program package [19] with the default convergence criteria without any constraint on the geometry [20]. Crystallographically obtained geometrical data of the molecules listed in Table 1 used for the optimization. The natural bonding orbitals (NBO) calculations [21] were performed using NBO 3.1 program as implemented in the Gaussian 09W package at the DFT/B3LYP/3-21G(*) level. The geometry-optimized structure, total molecular energy, dipole moment, and Mulliken charges were obtained from the optimization output.

3. Result and Discussion

3.1. Syntheses of 5-Arylidene-2,2-dimethyl-1,3-dioxane-4,6-diones (2)

Meldrum's acid (1 equi) and 2-formylphenoxyaliphatic acid (1a, 1 equi) were added to water at 80 ^{o}C. 2-Formylphenoxyacetic acid and Meldrum's acid were completely miscible in hot water and yellow solid of 2a was precipitated out within 5 min. This reaction was categorized as 'in-water process' [11, 12, 22] (Scheme 1).

A thorough literature survey showed that the same product was observed from equimolar mixture of Meldrum's acid and aromatic aldehyde(s) with acid [9] or base [4] catalyst. F. Bigi *et al* [8] reported the condensation of Meldrum's acid with aromatic aldehyde(s) in water without any catalyst. But the reaction time (2h) [8] is higher than our reaction (5 min). This revealed that the 2-formylphenoxyacetic acid act as an *in-situ* Bronsted-Lowry acid catalyst. This was extended to other formylphenoxyaliphatic acids (Scheme 1).

3.2. Single crystal XRD studies

Compounds 2a, 2b, 2c, and 2d were crystallized using aqueous ethanol (1:1) under slow evaporation. The suitable crystals were collected and characterized by single crystal X-ray diffraction studies. The ORTEP views of the compounds are shown in Fig. 1. Compounds 2a.H_2O, 2b, and 2c were crystallized as triclinic system and 2d was crystallized as monoclinic system. Crystal data and structure refinement is shown in Table 1.

Systematic reflection conditions and statistical tests of the data suggested the centrosymmetric space group *P*-1 for 2a.H_2O and it was stabilized by H-bonding through water molecule (H7O-O20w is 1.737 Å, O4-H20Pw is 1.934 Å, and O6-H20Ow is 1.947Å). Etters graph set notation [23] for the monomer is $R_2^2(13)$ and the dimer is $R_2^1(12)$ for 2a.H_2O (Fig. 2). However, other three compounds 2b, 2c, and 2d were crystallized as like normal acid dimer synthon through intermolecular H-bonding (Fig. 2) and the Etter's graph set notation is $R_2^2(8)$. But the O-H bond length is varied *i.e* 1.810 Å (2b), 1.758 Å (2c), and 1.819 Å (2d). Compound 2c alone have π-π interactions (3.594 Å and 3.793 Å) (Fig. 3). Other compounds did not have π-π interactions. But compounds 2a (C5-H5B---Ar is 3.403 Å), 2b (C7-H7---Ar is 3.401 Å), and 2d (C14-H14B---Ar is 3.150 and C6-H6A---Ar is 4.085 Å) have C-H---π interactions.

Planarity of olefin substitution showed that the proton (H7) and aromatic ring are in the same plane but the other end of olefin is substituted with Meldrum's acid which was not in the same plane (C7C3C4-C7C3C2 for 2a is 11.60 Å, 2b is 6.24 Å, 2c is 2.53 Å, and 2d is 3.41 Å). The planarity of olefinic proton (C3C7H7A) and aryl ring (C8C9C10C11C12C13) showed that 2a (37.74 Å) is higher and 2b (4.02 Å) is lower, and other 2c (26.93 Å) and 2d (14.20 Å) are moderate.

3.3. DPPH Radical Scavenging Activity

The role of antioxidant is to scavenge free radical. Mechanism through which this is achieved is by donating hydrogen to free radical in its reduction to an unreactive species. Addition of hydrogen would remove the odd electron feature which is responsible for radical reactivity. The hydrogen donating activity, measured using DPPH (1,1-diphenyl-2-picrilhydrazyl) radical as hydrogen acceptor, showed a significant association could be found between the concentration of novel molecule and percentage of inhibition. The free radical scavenging activity of the compounds 2a-2d was tested using DPPH model system and the results are presented in Table 2. It reveals that, 2c have better scavenging activity at 25 ppm concentration (82.68±0.52) followed by 2b.

3.4. In-vitro anticancer activity

We screened the growth inhibition or antiproliferative effects of 2a-2d on the cancer cell line A431, AGS, and U373MG using MTT assay [11, 12]. These compounds (2a-2d) have IC_{50} more than 300 µM on AGS and U373MG cell lines. They have lower antiproliferative effects on A431 cell line. The data showed that 2a (87.6 µM) had lower IC_{50} than other compounds 2b (96.48 µM), 2c (104.90 µM), and 2d (128.36 µM).

3.5. Theoretical Studies

The first task for the computational work is to determine the optimized geometries of the studied molecules with the help of the single crystal XRD structures. Gas phase geometry optimizations performed starting from the crystal structure 2a.H_2O at the B3LYP/3-21G(*) level of theory. Water molecule was excluded from the structure of 2a.H_2O before optimization. Similarly the ground state geometrical optimization done to 2b, 2c, and 2d using the same method. The optimized structure of 2a, 2b, 2c, and 2d are shown in Fig. 4. The most relevant structural parameters - bond lengths, bond angles, and dihedral angles of 2a, 2b, 2c, and 2d

determined by the same method are given in Table 3. The calculated geometrical parameters show good correlation with experimental values and can be as a foundation to calculate the other parameters such as total energy, dipole moment, NBO, HOMO, LUMO, and electrostatic potential map for the molecules. The results revealed that the optimized parameters are slightly different compared to the experimental parameters (Table 3) due to the fact that the theoretical calculations belong to isolated molecules in a gaseous state and the experimental results belong to molecules in the solid state.

3.6. Natural bond orbital (NBO) analysis

It is well-known that NBO analysis provides an efficient method for studying intra- and inter-molecular bonding and interaction among bonds and also provides a convenient basis for investigating charge transfer or conjugative interaction in molecular systems [24]. Delocalization of electron density between occupied Lewis type (bonded or lone pair) NBO orbitals and formally unoccupied (antibonded or Rydgberg) non-Lewis NBO orbitals correspond to a stabilizing donor–acceptor interaction. Table 4 shows NBO results showing the formation of Lewis and non-Lewis orbitals of 2a and the data of other molecules are given in the supplementary information (*vide* supporting information, Table S1-S3).

The bonding orbital for C28-O34 has 34.04% C28 character in a $sp^{1.94}$ hybrid and has 65.96% O34 character in a $sp^{1.61}$ hybrid orbital of 2a. The bonding orbital for C31-O37 has 33.05% C31 character in a $sp^{2.03}$ hybrid and has 66.95% O37 character in a $sp^{1.63}$ hybrid orbital of 2b. The bonding orbital for C28-O34 has 34.02% C28 character in a $sp^{1.94}$ hybrid and has 65.98% O34 character in a $sp^{1.61}$ hybrid orbital of 2c. The bonding orbital for C31-O37 has 32.82% C31 character in a $sp^{2.05}$ hybrid and has 67.18% O37 character in a $sp^{1.62}$ hybrid orbital

of 2d. The C=O bond possess more p-character than s-character for all the molecules in the alkyl chain part [25].

In order to investigate the intermolecular interactions, the stabilization energies of 2a were computed by using second-order perturbation theory. For each donor NBO(i) and acceptor NBO(j), the stabilization energy $E^{(2)}$ associated with electron delocalization between donor and acceptor is estimated as [26,27].

$$E^{(2)} = \Delta E_{ij} = q_i \frac{\mathrm{F(i,j)}^2}{\varepsilon_j - \varepsilon_\mathrm{i}}$$

where q_i is the donor orbital occupancy, ε_i and ε_j are diagonal elements (orbital energies), and $F(i, j)$ is the off-diagonal NBO Fock matrix element. The results of second-order perturbation theory analysis of the Fock Matrix at the B3LYP/3-21G(*) level of theory are presented in Table 5 (vide supporting information, Table S4-S6).

From Table 6, the intermolecular hyperconjugative interactions of the π-π* transitions (C3–C13, C15–C16, C18–C20, C22-C24) in -C=C- group and benzene ring lead to strong delocalization for 2a and 2b. At *para*-position the cancellations of hyperconjugation through the cyclohexane ring with the absence of interaction energy in NBO analysis. Therefore, the substituent at *ortho*-position is more delocalized compared to *para*-position.

The interaction between the O-atom (-OH group) lone pair and C-O antibonding orbital gives a strong stabilization of 46.18 (2a), 48.74 (2b), 35.61 (2c), and 47.44 Kcal mol^{-1} (2d) respectively. The interaction energy ($E^{(2)}$) of *ortho*-position is larger than that of *para*-position. The larger the $E^{(2)}$ value, the more intensive is the interaction between electron donors and electron acceptors, i.e., the more donating tendency from electron donors to electron acceptors, the greater the extent of conjugation of the whole system. Therefore we have concluded from the NBO analysis that the π-bonding orbital nature is more delocalized at *ortho*-position.

The role of antioxidant is to scavenge free radical. Mechanism through which this is achieved is by donating hydrogen to free radical in its reduction to an unreactive species. Addition of hydrogen would remove the odd electron feature which is responsible for radical reactivity. The hydrogen donating activity, measured using DPPH (1,1-diphenyl-2-picrilhydrazyl) radical as hydrogen acceptor (Scheme 2). The hydrogen donating activity of compounds (2) is studied by NBO analysis. Compounds (2) have three active H-atoms, carboxylic O7-H7, olefinic C7-H7, and methylene C17-H17. In which, O7-H7 (ED_{energy} for 2a is 1.98992, 2b is 1.98850, 2c is 1.98982, and 2d is 1.99017 a.u.) have high energy than C7-H7 (ED_{energy} for 2a is 1.96903, 2b is 1.97072, 2c is 1.97192, and 2d is1.97105 a.u.) and C14-H14a (ED_{energy} for 2a is 1.97594, 2b is 1.98824, 2c is 1.97551, and 2d is 1.98785 a.u.) (*vide* supporting information). This reveals that the carboxylic O-H bond has high energy and more reactive. So the liberated H-atom radical is from carboxylic O-H bond in 2. The bond energy of O7-H7 bond of 2c is high which is confirmed by its experimental result (Table 2).

The *in-situ* Bronsted acid catalyzed reaction of the Knoevenagel condensation was also confirmed by the NBO analysis. 2-Formylphenoxyacetic acid and meldrums acid is taken as a model for the formation of 2a. Scheme 3 shows the possible reaction mechanism for the formation of 2a. Starting materials and intermediates (I-IV) are optimized using B3LYP/3-21G(*) (*vide* supporting information for the optimized structure I-IV and tables). Both C5-H11 and C5-C6 bonds have an electron density acceptor character (ED_{energy} for C5-H11 is 1.96561 and C5-C6 is 1.98348 a.u.) in methylene carbon of Meldrum's acid (keto-form) where C5 acts as nucleophilic cite. The carbonyl (C13-O14) bond has electron donating character (ED_{energy} is 1.99642 a.u.) whereas carbon (C13) acts as an electrophilic cite in 2-fromylphenoxyacetic acid. The electron density on O19-H37 (ED_{energy} is 1.98817 a.u.) in intermediate-III is analyzed. This

bond energy shows oxygen atom act as an electron pair acceptor which accept electrons from H11. The bond breaking and making in intermediate IV is found using NBO analysis. The liberated water molecule is found on the C11-O18 (ED_{energy} is 1.99251 a.u.) due to high bond energy. The liberation of water molecule from carbon atom (C11) induces the liberated H-atom from C5 atom (C5-H20, ED_{energy} is 1.92918 a.u.). Both carbon atoms [C5 ($sp^{3.70}$) and C11($sp^{4.19}$)] have high energy and need to stabilize by changing their hybridization leads to give 2a (ED_{energy} of C3-C7 is 1.97339 a.u, C30 ($sp^{1.62}$) and C7 ($sp^{1.66}$) (Table 4). The reactivity of formylphenoxyaliphatic acids are found using the bond energy of carbonyl C7-O8 bond in intermediate II [ED_{energy} is 1.99722 (IIa), 1.99723 (IIb), 1.99363 (IIc), and 1.99363a.u (IId)] (*vide* supporting information for NBO of IIb-c). These bond energy values reveal that ortho isomers (IIa and IIb) have same bond energy and higher energy than para isomers (IIc and IId). This reveals that ortho isomers have high reactivity with Meldrum's acid than para isomers.

3.7. Molecular Electrostatic Potential (MEP)

Molecular electrostatic potential (MEP) at a point in the space around a molecule gives an indication of the net electrostatic effect produced at that point by the total charge distribution (electron + nuclei) of the molecule and correlates with dipole moments, electronegativity, partial charges and chemical reactivity of the molecules. It provides a visual method to understand the relative polarity of the molecule. The different values of the electrostatic potential represented by different colours; red represents the regions of the most negative electrostatic potential, white represents the regions of the most positive electrostatic potential and blue represents the region of zero potential. Potential increases in the order red < green < blue < pink < white. It can be seen that the negative regions are mainly over the O3 atom. The negative (red colour) regions of MEP were related to electrophilic reactivity and the positive (blue colour) ones to nucleophilic

reactivity. The negative electrostatic potential corresponds to an attraction of the proton by the aggregate electron density in the molecule (shades of red), while the positive electrostatic potential corresponds to the repulsion of the proton by the atomic nuclei (shades of blue) [11,12].

Figure 5 (2a.H_2O) shows the negative (red) region is localized on the carbonyl oxygen atoms (O3, O4, and O6) and oxygen from water (O20) with minimum value of -0.06726 a.u. However, positive (light blue) region is localized on water containing hydrogen atoms, with a maximum value of 0.06726 a.u. and the green represents regions of zero potential. Therefore, Figure 5 confirms the existence of an intermolecular O-H---O interactions. This was confirmed from the single crystal XRD studies (Fig. 1a). Without water molecule the positive (blue) region is located on carboxylic acid hydrogen atom, the maximum and minimum potential value for 2a is -0.08276 and 0.08276 a.u. This confirms the presence of water increases the stability of 2a.

The MEP of 2b-2d (*vide* supporting information, Fig. S1), the negative (red) region is positioned on the carbonyl oxygen atoms and the maximum positive (blue) region on carboxylic acid hydrogen atom. This confirms the existence of an intermolecular O-H---O interactions. Figure 1 confirmed the intermolecular H-bonding was observed in single crystal XRD. The MEP of 2c showed the very low amount of positive and negative region on aromatic ring, this confirmed the presence of π-π interactions.

These sites give information concerning the region from where the compound can have intermolecular interactions. Figure 5 provides a visual representation of the chemically active sites and comparative reactivity of atoms. It may see that, a region of zero potential envelopes the π-system of the aromatic rings, leaving a more electrophilic region in the plane of hydrogen atoms in these molecules [28].

3.8. Frontier Molecular Orbitals (FMO)

HOMO and LUMO energies are very important parameters in quantum chemistry using which one can determine the way the molecule interacts with other species; hence, they are called the frontier orbitals. HOMO, which can be thought of as the outermost orbital containing electrons, tends to give these electrons and acts as an electron donor. On the other hand; LUMO can be thought as the innermost orbital containing free places and accepts electrons [29]. The highest occupied molecular orbital (HOMO) and lowest unoccupied molecular orbital (LUMO) of the derivatives are shown in Fig. 6. We have investigated the electronic structure of the compounds 2a-2d using the same DFT method (Table 6). The electron density of HOMO and LUMO is same as for all derivatives. The total energy and HOMO-LUMO energy gap is nearly same for all derivatives. Among these, 2d have higher dipole moment than other derivatives which indicate that the 2d have more polar compound than the others.

3.9. Atomic charges

Mulliken net charges and natural atomic charges are calculated at the DFT level with the 3-21G(*) basis set in gas phase using Gaussian 09W for all molecules. Mulliken net charges and natural atomic charges of 2a are shown in Fig. 7 (vide supporting information for other molecules, Fig.S2, Table S7). As can be seen in Fig. 7, all the hydrogen atoms have a net positive charge. Moreover, Mulliken net charges and natural atomic charges show that the H36 atom has higher positive atomic charges [0.362092 (0.51008) for 2a, 0.382073 (0.50466) for 2b] than the other hydrogen atoms. This is due to the presence of electronegative oxygen atom (O35) of the carboxylic acid group; the hydrogen atom (H36) attracts the positive charge from the oxygen atom (O35). The atomic charges at the sites of C2 atom attached to the O31 atom are more positive because of the electron withdrawing nature of the O-atom. The presence of high

negative charge on O-atom and net positive charge on H-atom may suggest the formation of intermolecular interaction in solid forms [30].

Conclusion

Self-catalysted, in-water Knoevenagel condensation of 2-[{(2,2-dimethyl-4,6-dioxo-1,3-dioxan-5-ylidene)methyl}phenoxy]aliphatic acids derived from Meldrum's and formylphenoxyaliphatic acid(s) have been reported. 2-formylphenoxyaliphatic acids act as an *in-situ* Bronsted-Lowry acid catalyst. We investigated the structures of theses derivatives by single crystal X-ray technique. Compounds 2b, 2c, and 2d were crystallized like normal acid dimer synthon through intermolecular H-bonding. Compounds displayed better DPPH radical scavenging activity. HOMO-LUMO energy gap confirms that the highest stability of compounds. MEP, NBO, and atomic charge confirmed the intermolecular interactions of compounds.

Acknowledgements

One of the authors (G.S. Suresh Kumar) thanks Ms. K. Ramalakshmi, Plantation Products Spices and Flavour Technology Department, Central Food Technological Research Institute, Council of Scientific and Industrial Research (CSIR), Mysore, India. CDRI, Lucknow, India is acknowledged for the spectral studies.

Reference

[1] M. Orio, D.A. Pantazis, F. Neese, Photosynth Res, 102 (2009) 443.

[2] (a) M.E. Zandler, F.D'Souza, C.R. Chimie, 9 (2006) 960;

(b) V.T. Yilmaz, S. Hamamci, S. Gumus, O. Buyukgungor, J. Mol. Str. 794 (2006) 142;

(c) J. Pina, J.S. Seixas de Melo, R.M.F. Batista, S.P.G. Costa, and M.M.M. Raposo, Phys. Chem. Chem. Phys., 12 (2010) 9719;

(d) C. Yuksektepe, N. Caliskan, I. Yilmaz, A. Cukurovali, J. Chem. Crystallogr. 40 (2010) 1049;

[3] (a) A.C. Razus, L. Birzan, L. Cristian, V. Tecuceanu, ARKIVOC, (xi) (2009) 31;

(b) S. Gao, T. Tzeng, Y.T. Lan, J.T. Liu, C.F. Yao, ARKIVOC, (xii) (2009) 347;

(c) B. C. Chen, Heterocycles 32 (1991) 529;

(d) H.A.A. Medien, Z. Naturforsch. 57b, (2002) 1320.

[4] (a) D. Davidson, S. A. Bernhard, J. Am. Chem. Soc. 70 (1948) 3426;

(b) E.J. Corey, J. Am. Chem. Soc. 74 (1952) 5897;

(c) S. Shital; R. Gajanan; K. Arjun; K. Santosh; S. Rajashri, Helvetica Chimica Acta 94(11) (2011) 1943;

(d) S.S. Shindhalkar, B.R. Madje, and M.S. Shingare, Indian J. Chem., 45B (2006) 2571.

[5] (a) G.A. Kraus, M.E. Krolski, J. Org. Chem. 51 (1986) 3347;

(b) P. Scuster, O.E. Polansky, F. Wessely, Monatsch. Chem. 95 (1964) 53.

[6] P.S. Rao, R.V. Venkataratnam, Indian J. Chem. B, 32 (1993) 484.

[7] J.A. Hedge, C.W. Kruse, H.R. Snyder, J. Org. Chem., 26 (1961) 3166.

[8] F. Bigi, S. Carloni, L. Ferrari, R. Maggi, A. Mazzacani, and G. Sartori, Tetrahedron Lett., 42 (2001) 5203.

[9] T. Murase, Y. Nishijima, and M. Fujita, J. Am. Chem. Soc., 134 (2012) 162.

[10] (a) V. Bala, Y.S. Chhonker, S.R. Hashim, Asian J. Chem. 22 (5) (2010) 3447;

(b) G.S. Suresh Kumar, P.G. Seethalakshmi, N. Bhuvanesh, S. Kumaresan, J. Mol. Str. 1034 (2013) 302;

(c) G.S. Suresh Kumar, P.G. Seethalakshmi, D. Sumathi, N. Bhuvanesh, S. Kumaresan, J. Mol. Str. 1035 (2013) 476;

(d) G.S. Suresh Kumar, P.G. Seethalakshmi, N. Bhuvanesh, S. Kumaresan, J. Mol. Str. 1050 (2013) 88;

(e) G.S. Suresh Kumar, A. Antony Muthu Prabhu, P.G. Seethalaksmi, N. Bhuvanesh, S. Kumaresan, Spectrochim. Acta, 101A (2013) 254.

[11] G.S. Suresh Kumar, A. Antony Muthu Prabhu, P.G. Seethalaksmi, N. Bhuvanesh, S. Kumaresan, Spectrochim. Acta, 123A (2014) 249.

[12] G.S. Suresh Kumar, A. Antony Muthu Prabhu, P.G. Seethalaksmi, N. Bhuvanesh, S. Kumaresan, J. Mol. Str., 1059 (2014) 51.

[13] (a) G.S. Suresh Kumar, S. Kumaresan, J. Chem. Sci. 124 (4) (2012) 857;

(b) B.S. Furniss, A.J. Hannaford, P.W.G. Smith, R. Austin, Vogel's textbook of practical organic chemistry, Longman Scientific and Technical, V edition (1989) 1160.

[14] Bruker APEX2, SAINT and SADABS, Bruker AXS Inc., Madison, Wisconsin, USA, 2008.

[15] G.M. Sheldrick, Acta Cryst. A 64 (2008) 112.

[16] A.L. Spek, Acta Cryst. D 65 (2009) 148.

[17] L.J. Farrugia, POV-Ray – 3.5, Glasgow University, Australia, 2003.

[18] (a) M.S. Blois, Nature 4617 (1958) 1199;

(b) K. Ramalakshmi, G. Hithamani, K.R. Asha, L.J. Mohan Rao, Int. J. Food Sci. Technol. 46 (2011) 109.

[19] Gaussian Inc., Gaussian 09 Program, Gaussian Inc., Wallingford, 2004.

[20] H.B. Schlegel, J. Comput. Chem. 3 (1982) 214.

[21] E.D. Glendening, A.E. Reed, J.E. Carpenter, F. Weinhold, NBO Version 3.1, TCI, University of Wisconsin, Madison, 1998.

[22] R.N. Butler, A.G. Coyne, Chem. Rev. 110 (2010) 6302.

[23] (a) M.C. Etter, J.C. MacDonald, J. Bernstein, Acta Cryst. B46 (1990) 256;

(b) M.C. Etter, Acc. Chem. Res. 23 (1990) 120;

(c) J. Bernstein, R.E. Davis, L. Shimoni, N.L. Chang, Angew. Chem. Int. Ed. Engl. 34 (1995) 1555;

(d) M.C. Etter, J. Phys. Chem. 95 (1991) 4601.

[24] M. Snehalatha, C. Ravikumar, I. Hubert Joe, N. Sekar, V.S. Jayakumar, Spectrochim. Acta 72A (2009) 654.

[25] K. Carthigayan, V. Arjunan, R. Anitha, S. Periandy, S. Mohan, J. Mol. Struct., 1056 (2014) 38.

[26] D.W. Schwenke, D.G. Truhlar, J. Chem. Phys. 82 (1985) 2418.

[27] M. Gutowski, G. Chalasinski, J. Chem. Phys. 98 (1993) 4728.

[28] V.P. Gupta, A. Sharma, V. Virdi, V.J. Ram, Spectrochim. Acta 64A (2006) 57.

[29] G. Gece, Corros. Sci. 50 (2008) 2981.

[30] Li Xiao-Hong, Liu Xiang-Ru, Zhang Xian-Zhou, Comput. Theor. Chem. 969 (2011) 27.

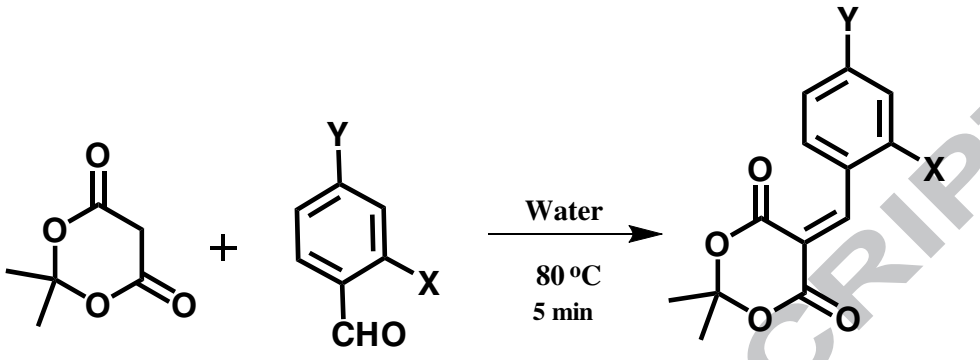

Scheme 1. Condensation of Meldrum's acid and formylphenoxyacetic acid.

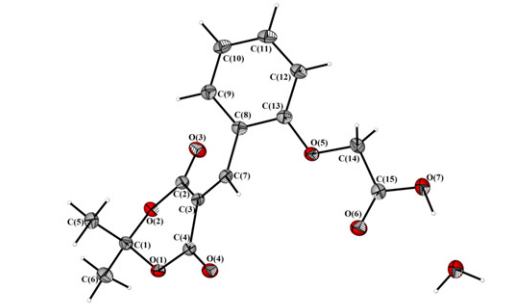

(a)

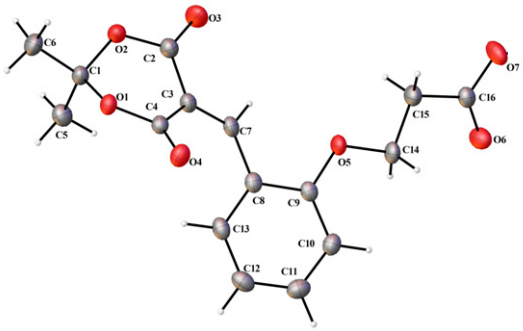

(b)

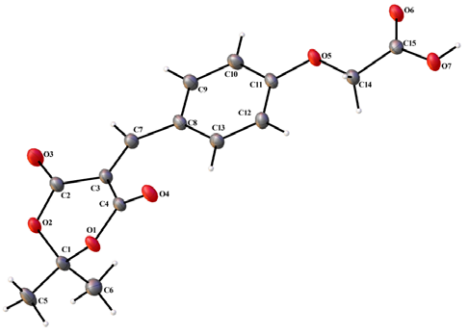

(c)

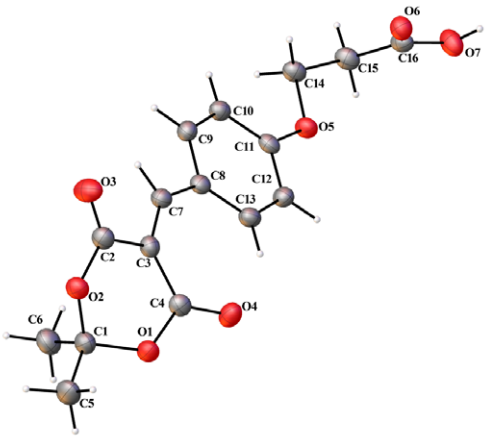

(d)

Fig. 1. ORTEP view of (a) **2a.H$_2$O**, (b) **2b**, (c) **2c**, and (d) **2d.**

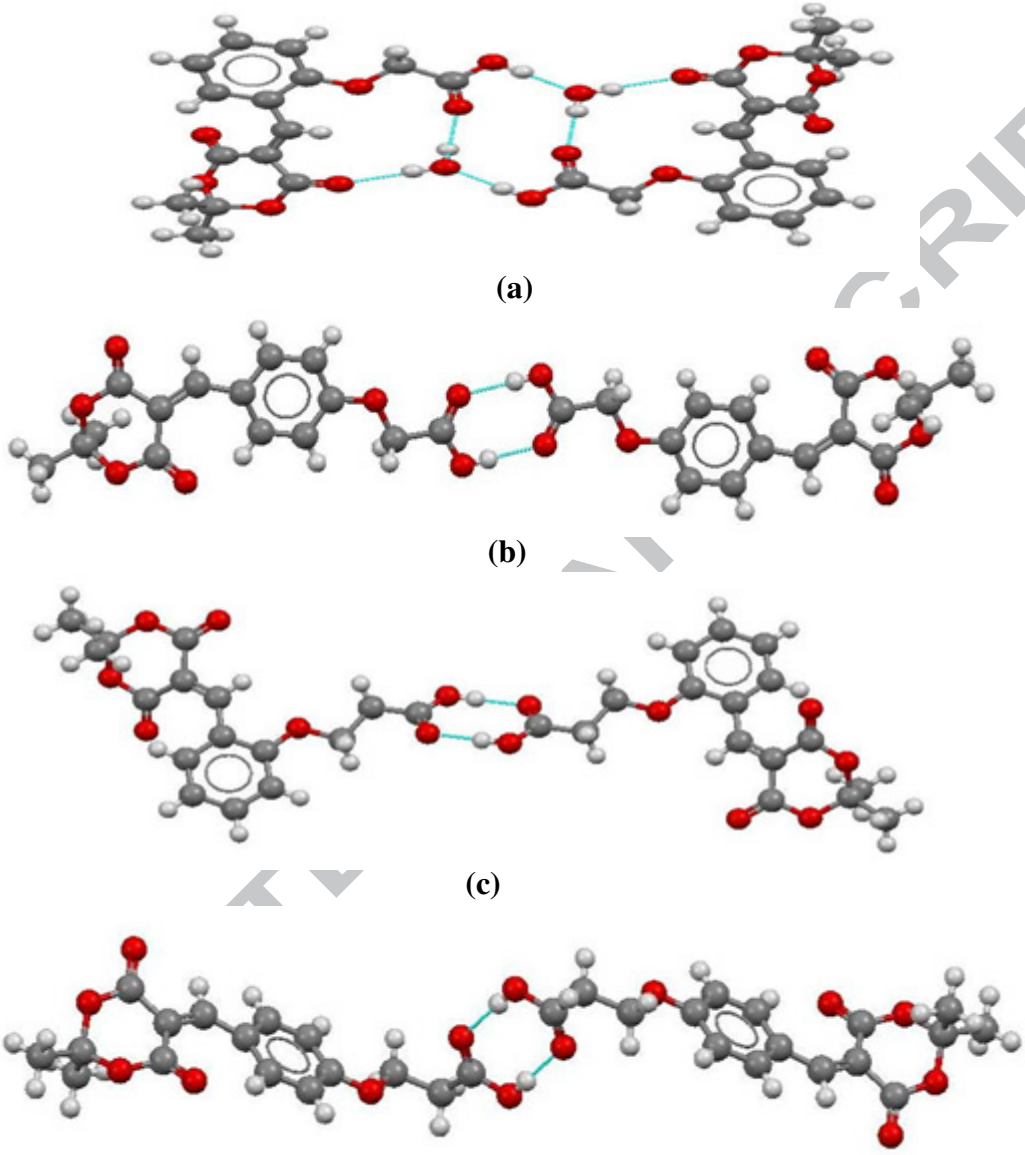

Fig. 2. Hydrogen bonding o... ...H_2O, (b) **2b**, (c) **2c**, and (d) **2d.**

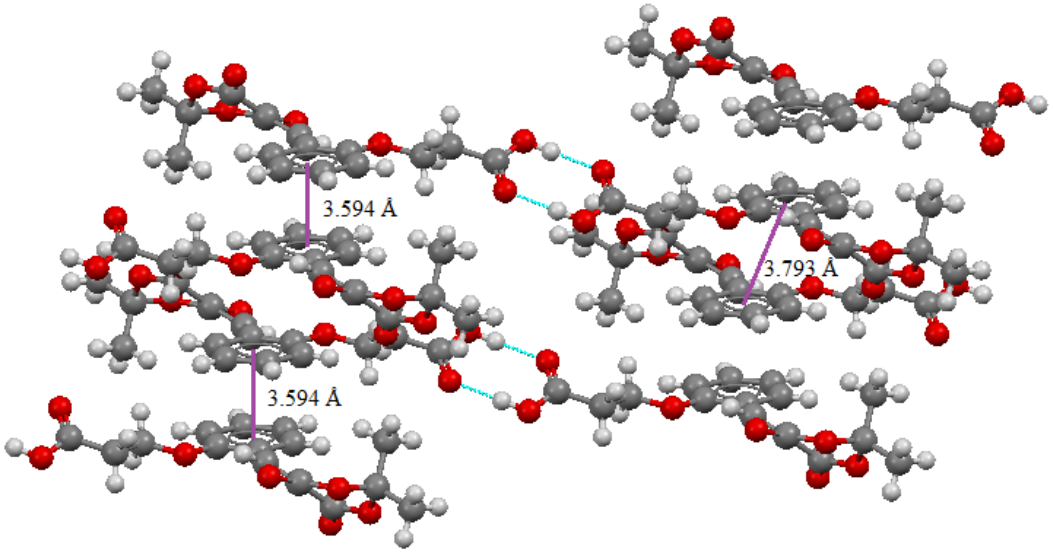

Fig. 3. π-π interactions of **2c.**

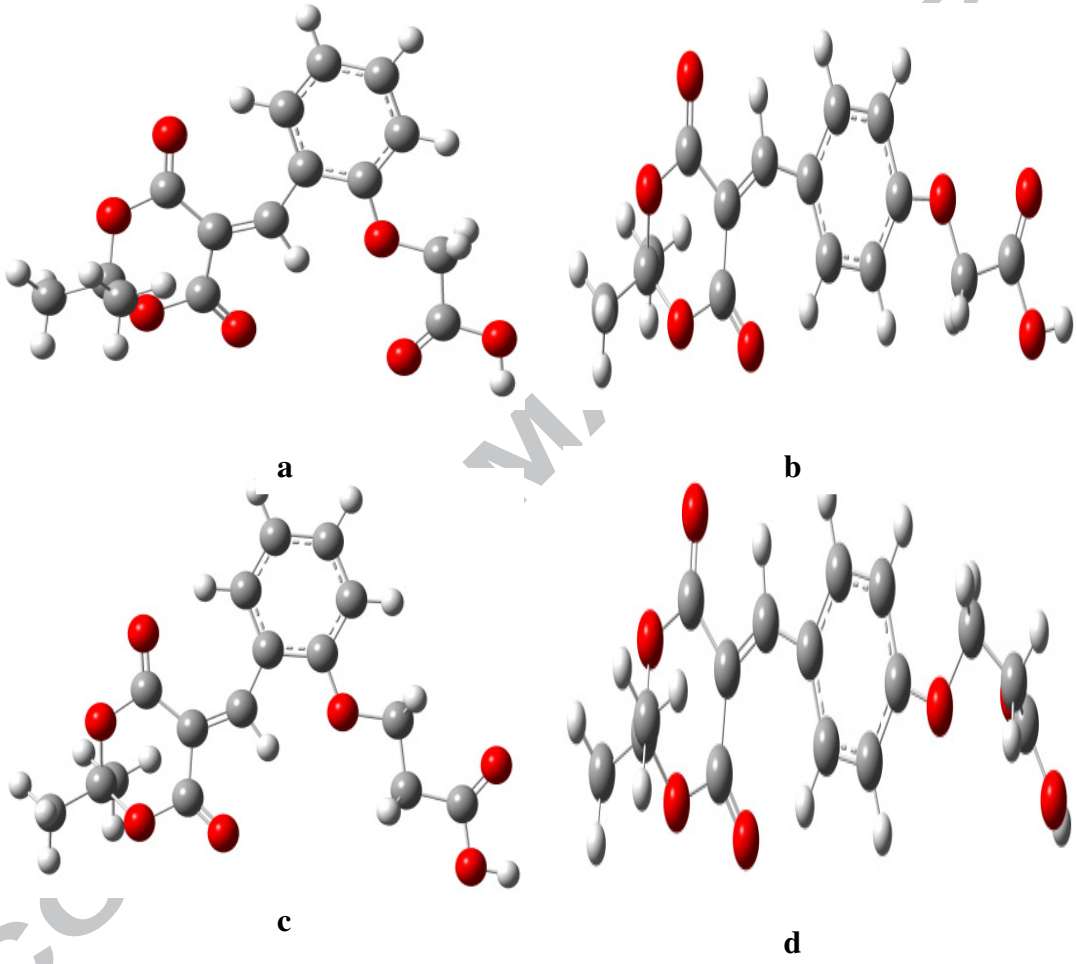

Fig. 4. The optimized structure of (a) **2a**, (b) **2b**, (c) **2c**, and (d) **2d.**

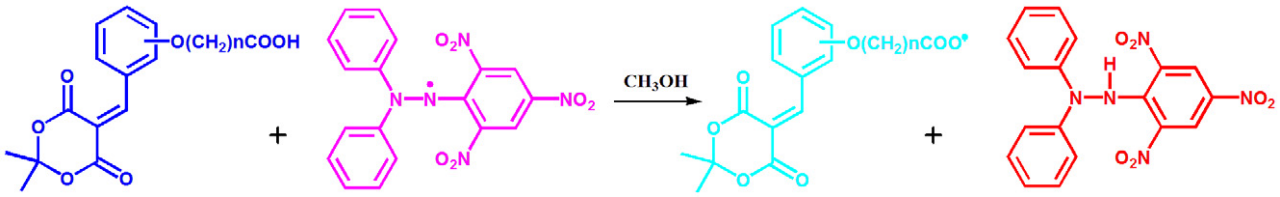

Scheme 2. DPPH radical scavenging reaction of **2**

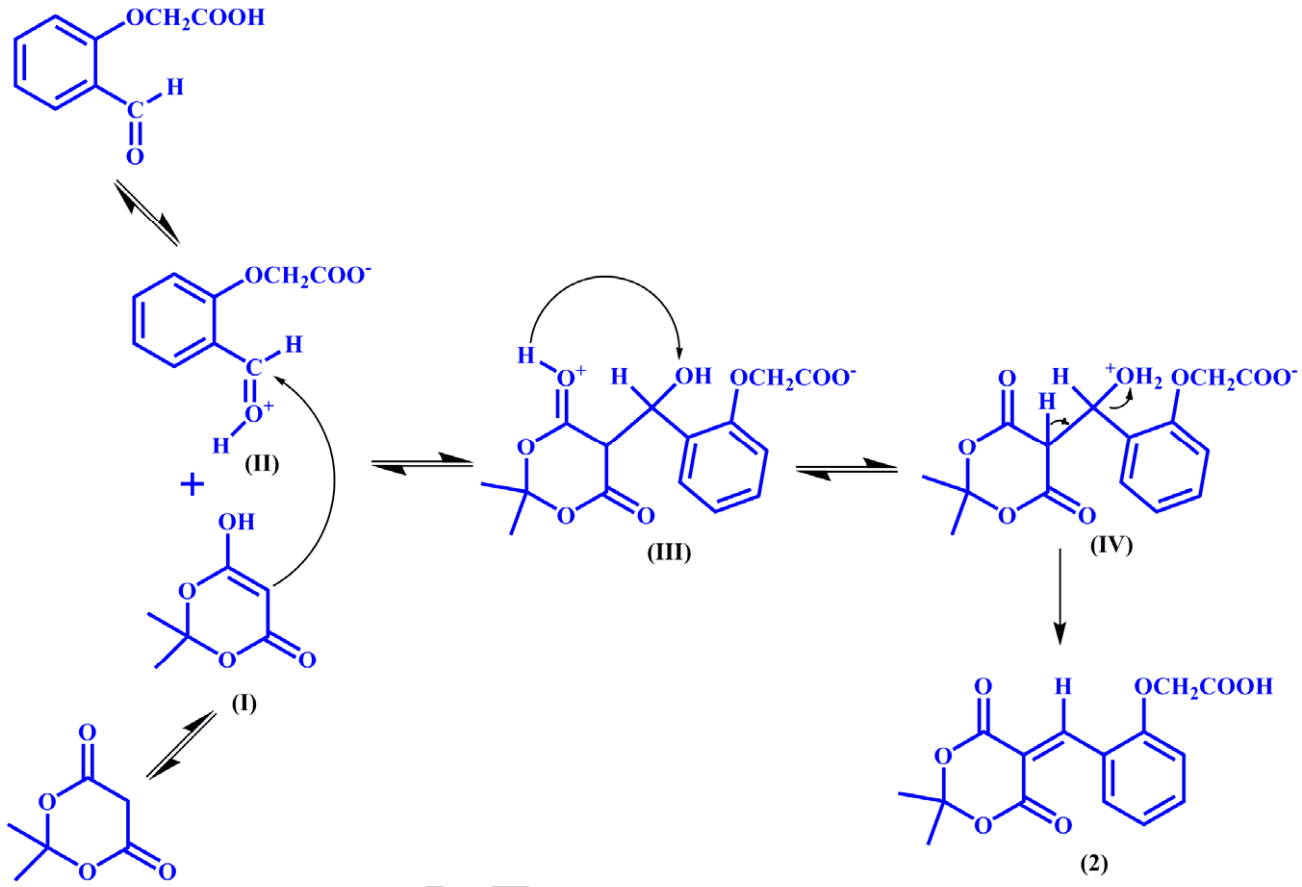

Scheme 3. Possible reaction mechanism of the formation of **2a**.

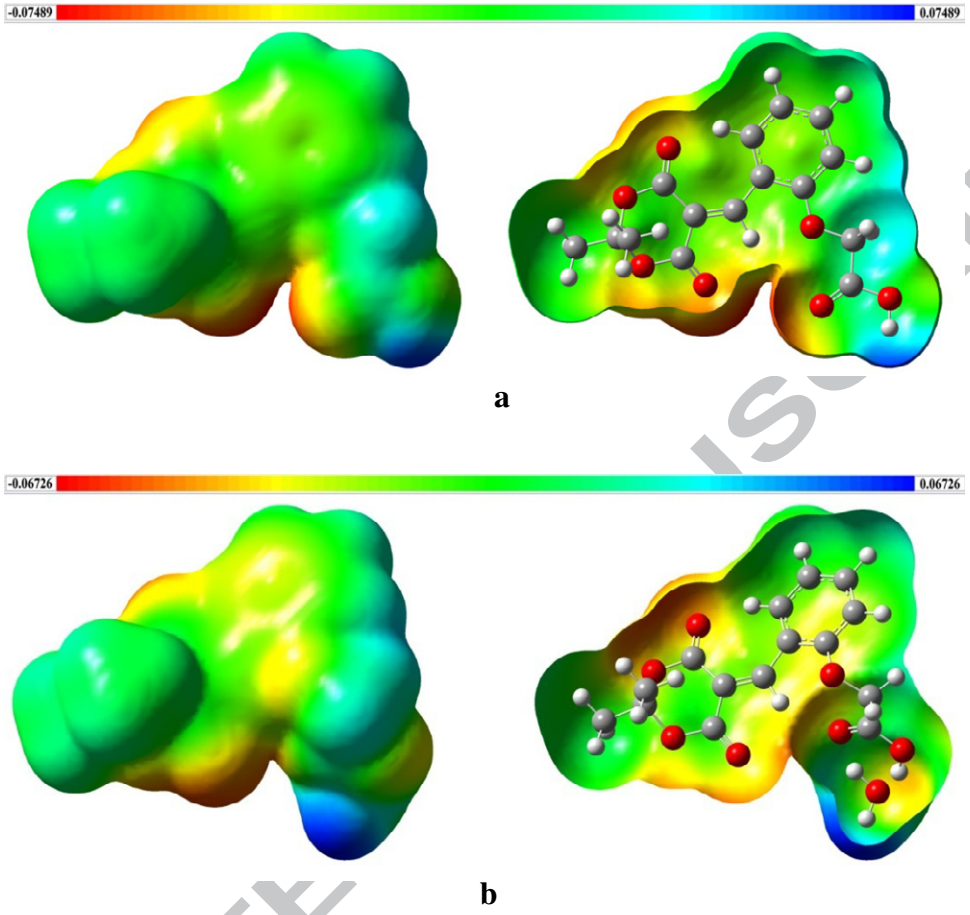

Fig. 5. The Molecular Electrostatic Potential (MEP) map of (a) **2a** and (b) **2a. H_2O.**

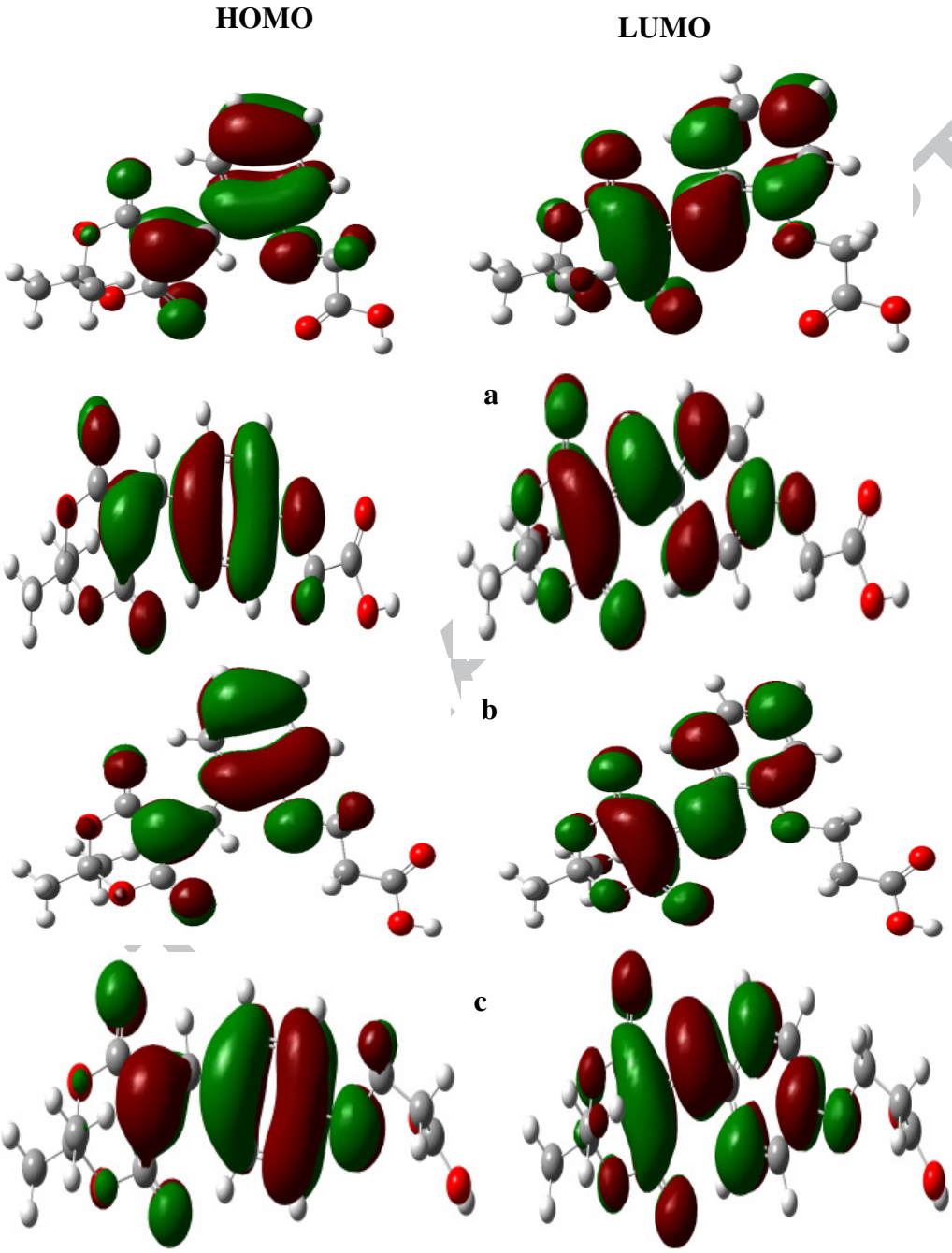

Fig. 6. The HOMO, LUMO energy st e of (a) **2a**, (b) **2b**, (c) **2c**, and (d) **2d.**

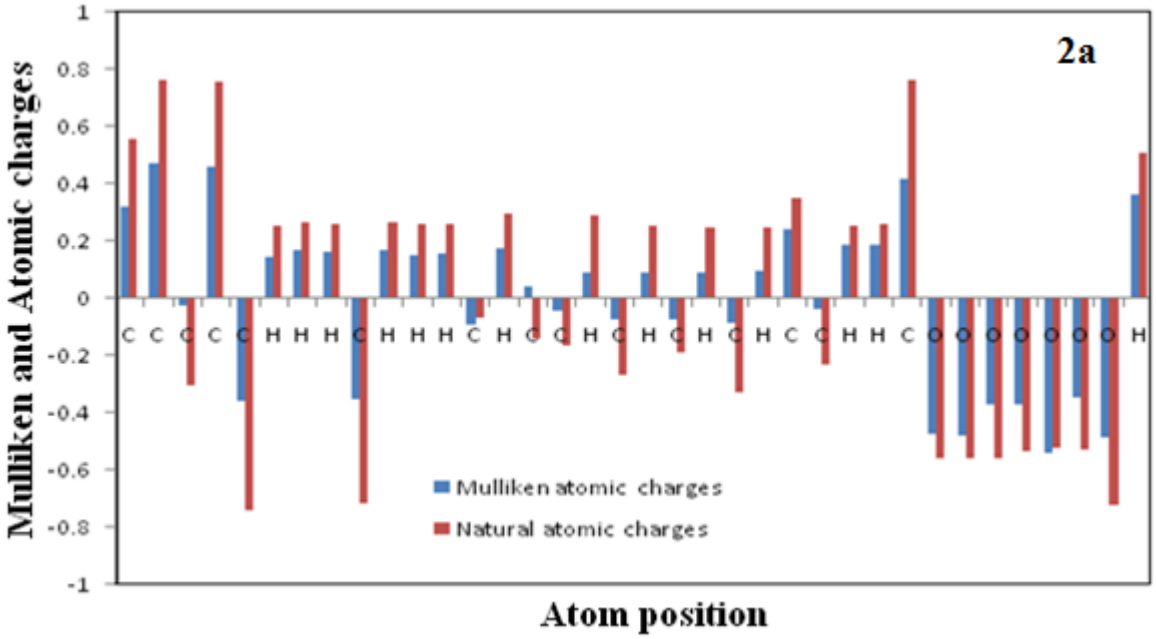

Fig. 7. Mulliken atomic charge and natural atomic charge plot of **2a**.